

Cavity-Mediated Strong Matter Wave Bistability in a Spin-1 Condensate

Lu Zhou¹, Han Pu², Hong Y. Ling³, and Weiping Zhang¹

¹*State Key Laboratory of Precision Spectroscopy, Department of Physics, East China Normal University, Shanghai 200062, China*

²*Department of Physics and Astronomy, and Rice Quantum Institute, Rice University, Houston, TX 77251-1892, USA and*

³*Department of Physics and Astronomy, Rowan University, Glassboro, New Jersey 08028-1700, USA*

We study matter wave bistability in a spin-1 Bose-Einstein condensate dispersively coupled to a unidirectional ring cavity. A unique feature is that the population exchange among different modes of matter fields are accomplished via the spin-exchange collisions. We show that the interplay between the atomic spin mixing and the cavity light field can lead to a strong matter wave nonlinearity, making matter wave bistability in a cavity at the single-photon level achievable.

PACS numbers: 03.75.Mn, 03.75.Kk, 42.50.Pq, 42.65.-k

The macroscopic nonlinear phenomena associated with ultracold atoms have become a main stream of research interest in the emerging field of atom optics [1]. Meanwhile they establish intimate connection of the new field to other branches of physics, such as nonlinear optics and condensed matter physics. One important aspect in the field is how to coherently manipulate the nonlinear behaviors of ultracold atomic ensembles for different purposes.

The ability of an optical cavity to provide feedback between input and output light fields can result in the modification of the atom-photon interaction in a highly nonlinear fashion. The exploration of such a nonlinear interaction for applications of both applied and fundamental interest has led to many exciting developments, including optical bistability, which was a subject of extensive study by the optics community in the 1980's, due mostly to the prospect of its use as an optical switch in all-optical computers [2]. In recent years, rapid technological advancement in cooling, trapping, and condensation of neutral atoms has brought new opportunities to cavity quantum electrodynamics (QED). A combination of cold atoms and large coherence couplings enables single-atom trajectories to be monitored in real time with high signal-to-noise ratio [3] while allows the vacuum Rabi splitting of a single trapped atom to be experimentally observed [4].

Instead of a *single* atom, more recent studies in cavity QED focus on cavity systems with a *collection* of ultracold atoms [6, 7, 8, 9, 10, 11], in which strong coupling of ultracold atomic gases to cavity optical field are realized. This allows us to enter a new regime of cavity QED, where a cavity field at the level of a single photon can significantly affect the collective motion of the atomic samples. This opens up new possibilities to manipulate the nonlinear dynamics of ultracold atomic gases with cavity-mediated nonlinear interaction.

So far the works involving in cavity with ultracold atomic gases have mainly focused on the interplay between the cavity field and the atomic external degrees of

center-of-mass motion [8, 9, 10, 11, 12, 13, 14, 15]. The role of internal spin degrees of ultracold atomic gases in the atom-cavity coupling has not yet been seriously explored. An intriguing property of spinor Bose-Einstein condensate (BEC) is that in addition to the repulsive binary collisions, atoms of different spin components can couple to each other via spin-exchange interactions, which give rise to spin mixing [16], a nonlinear dynamical phenomenon under intense theoretical [17, 18, 19] and experimental investigation [20, 21, 22, 23, 24]. In this work we propose a scheme to exploit the atom-cavity coupling to control the atomic spinor dynamics in a spinor BEC. In contrast to the existing works which focus primarily on optical bistability, here we pay particular attention to the matter-wave bistability. As we will show, the combination of cavity-induced phase shift and the intrinsic spin-exchange interaction of a spinor BEC leads to very strong matter-wave bistability, providing a new playground for exploring the spinor dynamics and cavity nonlinear optics.

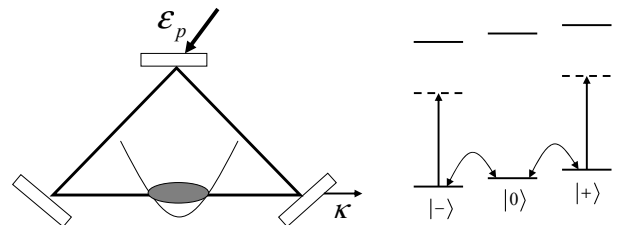


FIG. 1: Schematic diagram showing the system under consideration.

Our model — a spinor BEC with hyperfine spin $F = 1$ confined in a unidirectional ring cavity — is depicted schematically in Fig. 1. At zero temperature we assume single-mode approximation (SMA) that atoms in different spin states can be described by the same spatial wave function $\phi(\mathbf{r})$, then each spin component can be associated with an annihilation operator \hat{c}_α ($\alpha = \pm, 0$). A weak external magnetic field may be applied to break the de-

generacy and provide the quantization axis. The cavity is designed in a way that only a single traveling mode with frequency ω_c , described by an annihilation operator \hat{a} , interacts with the atoms. The cavity is driven by a coherent laser field with frequency ω_p and amplitude ε_p .

The Hamiltonian under the SMA can be written as

$$\hat{H} = \hat{H}_0 + \left[U_0 \left(\hat{c}_+^\dagger \hat{c}_+ + \hat{c}_-^\dagger \hat{c}_- \right) - \delta_c \right] \hat{a}^\dagger \hat{a} + i\varepsilon_p (\hat{a}^\dagger - \hat{a}),$$

with \hat{H}_0 describing the dynamics of spinor condensate

$$\begin{aligned} \hat{H}_0 = & \lambda_a \left(\hat{c}_+^\dagger \hat{c}_+^\dagger \hat{c}_+ \hat{c}_+ + \hat{c}_-^\dagger \hat{c}_-^\dagger \hat{c}_- \hat{c}_- + 2\hat{c}_0^\dagger \hat{c}_0 \hat{c}_+^\dagger \hat{c}_+ \right. \\ & + 2\hat{c}_0^\dagger \hat{c}_0 \hat{c}_-^\dagger \hat{c}_- - 2\hat{c}_+^\dagger \hat{c}_+ \hat{c}_-^\dagger \hat{c}_- + 2\hat{c}_0^\dagger \hat{c}_0 \hat{c}_+ \hat{c}_- + 2\hat{c}_+^\dagger \hat{c}_+ \hat{c}_- \hat{c}_0 \\ & \left. + q \left(\hat{c}_+^\dagger \hat{c}_+ + \hat{c}_-^\dagger \hat{c}_- \right) \right), \end{aligned}$$

here λ_a is the spin-dependent interaction coefficient [16] of the condensate. We denote q as the quadratic Zeeman shift. $\delta_c = \omega_p - \omega_c$ is the cavity-pump detuning. $U_0 = g^2 / (\omega_p - \omega_a)$, with g being the dipole coupling strength and ω_a the atomic transition frequency, characterizes the strength of the atom-photon coupling. We will assume that the photon frequency is sufficiently detuned away from the atomic transitions so that the atomic upper level can be adiabatically eliminated and the interaction between photon and atom is essentially of dispersive nature. We assume that the photons are π polarized which couple the atoms in the $F = 1$ ground-state manifold to the excited manifold with $F' = 1$. The transition selection rule is $\Delta m_F = 0$. However, since the transition $|F = 1, m_F = 0\rangle_g \rightarrow |F' = 1, m_F' = 0\rangle_e$ is forbidden, spin-0 level is not coupled by the photon. For simplicity, we also assume that the coupling strength between the cavity field and spin- \pm atoms are the same. We will treat the leakage of cavity photons phenomenologically by introducing a decay rate κ with typical values ~ 1 MHz. By contrast, the time scale for the atomic spin-mixing dynamics is much longer — the measured population oscillation frequency is below 10 Hz for ^{87}Rb [23] and around 50 Hz for ^{23}Na [24]. This separation of time scales allows us to assume that the cavity field always follows adiabatically the atomic dynamics

$$\hat{a} = \frac{\varepsilon_p}{\kappa - i \left[\delta_c - U_0 \left(\hat{c}_+^\dagger \hat{c}_+ + \hat{c}_-^\dagger \hat{c}_- \right) \right]}. \quad (1)$$

The corresponding Heisenberg equations of motion for the atomic field operators read

$$i\dot{\hat{c}}_\pm = \left[\hat{c}_\pm, \hat{H}_0 \right] + U_0 \hat{a}^\dagger \hat{a} \hat{c}_\pm, \quad i\dot{\hat{c}}_0 = \left[\hat{c}_0, \hat{H}_0 \right]. \quad (2)$$

Combining Eqs. (1) and (2), in the bad cavity limit one can find the effective Hamiltonian \hat{H}_{eff} which satisfies $i\dot{\hat{c}}_\alpha = \left[\hat{c}_\alpha, \hat{H}_{eff} \right]$

$$\hat{H}_{eff} = H_0 - \frac{\varepsilon_p^2}{\kappa} \tan^{-1} \left[\frac{\delta_c - U_0 \left(\hat{c}_+^\dagger \hat{c}_+ + \hat{c}_-^\dagger \hat{c}_- \right)}{\kappa} \right]. \quad (3)$$

In the following we adopt a mean-field treatment by replacing the operators \hat{a} and \hat{c}_α with the corresponding \mathcal{C} numbers $\alpha = \langle \hat{a} \rangle$ and $c_\alpha = \sqrt{N_\alpha} \exp(-i\theta_\alpha)$, where N_α and θ_α represent the number and phase of the bosonic field for the particles in the spin component α , respectively. We take advantage of the existence of two conserved quantities: the total atomic number $N = N_+ + N_- + N_0$ and magnetization $M = N_+ - N_-$, and simplify our problem into the one described by two variables: the normalized population in the spin-0 component $x = N_0/N$ and the relative phase $\theta = 2\theta_0 - \theta_+ - \theta_-$. The mean-field counterpart of the quantum effective Hamiltonian (3) read

$$\begin{aligned} \frac{H}{N\kappa} = & \bar{q}(1-x) + \bar{\lambda}_a x \left[1 - x + \sqrt{(1-x)^2 - m^2} \cos \theta \right] \\ & + U(x), \end{aligned} \quad (4)$$

with $U(x) \equiv \eta^2 \tan^{-1} [\bar{U}_0(1-x) - \bar{\delta}_c] / N$ and $m = M/N$ is the atomic polarization. We have defined other dimensionless parameters as

$$\bar{\lambda}_a = \frac{N\lambda_a}{\kappa}, \quad \bar{q} = \frac{q}{\kappa}, \quad \bar{U}_0 = \frac{NU_0}{\kappa}, \quad \eta = \frac{\varepsilon_p}{\kappa}, \quad \bar{\delta}_c = \frac{\delta_c}{\kappa}.$$

The equations of motion for x and θ read

$$\frac{dx}{d\tau} = 2\bar{\lambda}_a x \sqrt{(1-x)^2 - m^2} \sin \theta, \quad (5a)$$

$$\begin{aligned} \frac{d\theta}{d\tau} = & -2 \left(\bar{q} + \frac{\bar{U}_0 |\alpha|^2}{N} \right) \\ & + 2\bar{\lambda}_a \left[1 - 2x + \frac{(1-x)(1-2x) - m^2}{\sqrt{(1-x)^2 - m^2}} \cos \theta \right], \end{aligned} \quad (5b)$$

where $\tau = \kappa t$ is the dimensionless time.

From Eq. (5b) one can see that the cavity modifies the atomic dynamics in the same manner as the quadratic Zeeman terms \bar{q} , which will lead to redistribution of atomic population among different spin states through spin mixing. However, this cavity-induced effective Zeeman energy is dependent upon the atomic population distribution via Eq. (1). It is this inter-dependence of the atomic and photonic modes that leads to interesting nonlinear dynamics of this coupled system, which will be the focus of this work.

The dynamics of the system can be captured by the contour plot of the Hamiltonian H , which is intimately related to the fixed points (x_0, θ_0) given by the equilibrium solution of Eqs. (5). In this work, we only consider the anti-ferromagnetic atoms (^{23}Na) with $\bar{\lambda}_a > 0$. The ferromagnetic case is not qualitatively different. In the absence of the cavity field, the equilibrium solutions (x_0, θ_0) have been studied in [18, 25]. Besides the phase-independent solutions of $x_0 = 0$ and $x_0 = 1 - |m|$

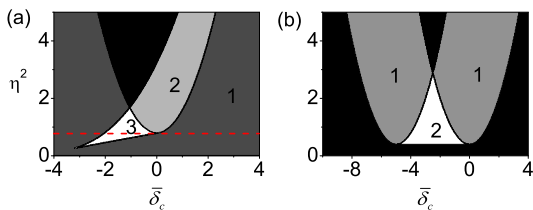


FIG. 2: (Color online) Phase diagram in the parameter space of $\bar{\delta}_c$ and η^2 for different type of solutions: (a) $\theta = 0$; (b) $\theta = \pi$. Different regions are differentiated by their colors and are labeled with the numbers of corresponding solutions. In the black region, no physical phase-dependent solutions can be found. The dimensionless parameters are estimated to be $\bar{\lambda}_a = 10^{-3}$, $\bar{q} = 2\bar{\lambda}_a$ and $\bar{U}_0 = -5$ [26], the other parameters are set as $m = 0$ and $N = 1000$. The red dashed line in (a) correspond to $\eta^2 = 0.8$.

for which the relative phase θ_0 is not well-defined, the spinor condensate system supports at most one phase-dependent solution with $\theta_0 = 0$ or π . The presence of the cavity field dramatically changes this property. The phase diagram identifying different types of solution is mapped out in the parameter space of η^2 and $\bar{\delta}_c$, as shown in Fig. 2. We can see that, in certain parameter regime, the number of different phase-dependent solutions can be more than one, different solution regimes of the coupling system can be crossed by varying $\bar{\delta}_c$ and η^2 . Since these two parameters are directly related to the pump laser, this means that the dynamical properties of the system can be easily manipulated by tuning the intensity or frequency of the pump laser field.

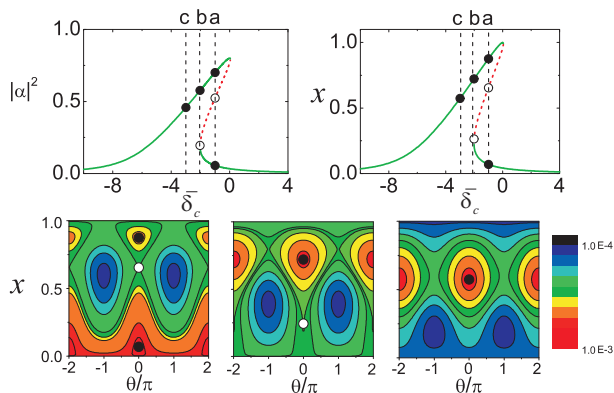


FIG. 3: (Color online) Upper panel: Mean intracavity photon number $|\alpha|^2$ and the normalized spin-0 population x versus cavity-pump detuning $\bar{\delta}_c$ for the steady-state solutions with $\eta^2 = 0.8$, corresponding to the red-dashed line in Fig. 2(a). The ones that represented by the red dotted lines correspond to dynamically unstable solutions. Lower panel: From left to right, the phase-space contour plot of H corresponding to different values of $\bar{\delta}_c$ marked in the upper panel as a, b and c, respectively.

Here we consider the case with the pump intensity η^2 fixed, by varying the cavity-pump detuning $\bar{\delta}_c$, the equilibrium properties of the system are changed, as shown in the red-dashed line in Fig. 2(a). The correspond-

ing phase-dependent fixed points are derived and the results are shown in Fig. 3. The system exhibits typical bistable behavior: For certain values of $\bar{\delta}_c$, it supports three stationary solutions. A standard linear stability analysis shows that in the region with three solutions, two of these are dynamically stable and the third one is dynamically unstable. Further insights can be gained by examining the corresponding contour plot of H (Fig. 3, lower panel). The unstable fixed points correspond to the saddle points in the contour plots.

The same hysteresis feature can also be identified from the mean-field energy diagram by the appearance of a swallowtail loop structure (the dots in Fig. 4). A quantum calculation involving a direct diagonalization of the effective Hamiltonian \hat{H}_{eff} confirms a well-known correspondence between the semiclassical and quantum energy levels [27], namely, in the bistable region the quantum spectrum (the solid lines in Fig. 4) exhibits a series of anticrossings and when connected, these anticrossings form the top segment of the swallowtail structure of the corresponding mean-field energy level. (In this example, we have, without loss of the essential physics, adopted a much smaller system so that the quantum calculation can be done within a reasonable computational time.)

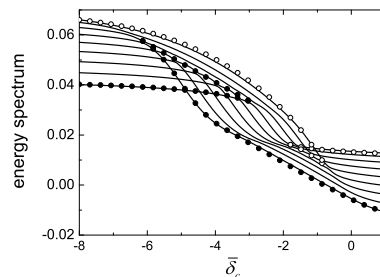


FIG. 4: Quantum and mean-field energy levels with $N = 20$, $m = 0.2$ and $\eta^2 = 0.02$, the other parameters are the same as before. The solid lines are quantum energy levels, the black dots refer to the mean-field energy levels with $\theta = \pi$, while the white dots refer to those with $\theta = 0$.

Let us now return to Fig. 3. As indicated in the upper panel of Fig. 3, both the cavity field and the atoms exhibit bistable behavior. The mean cavity photon number involved is always less than unity. Remarkably, such a small number of photons affect the whole condensate and lead to complete population redistribution among different internal atomic spin states, which can be readily observed in experiment. This behavior can be understood as following: The collective nature of the condensate greatly enhances the atom-photon coupling such that a single photon gives rise to a significant atomic phase shift, which in turn strongly modifies the population distribution among the spin states. Bistability results from the nonlinear feedback between photons and atoms.

It is interesting to compare our study with the experi-

mental work of Refs. [9, 11], where the motional degrees of freedom of ultracold atomic gases represent the source of nonlinearity affecting light-atom interactions. In their system the atomic zero-momentum mode and two side modes with momentum $\pm 2\hbar k$ (k is the cavity light wave vector) dominate the dynamics. The nonlinearity originates from the coherence between these modes which is induced by the coupling provided by the standing-wave cavity field [28]. Such a coupling is neither strong as it is provided by the weak cavity field, nor resonant as there is a detuning of $4\hbar\omega_{rec}$ with $\omega_{rec} = \hbar k^2/2m$ the atomic recoil frequency. In these systems, optical bistability of low photon numbers is possible and is indeed observed. In principle, atomic population in different motional states should also exhibit bistability. However, such matter-wave bistability will be difficult to observe as it is not easy to measure atomic population of different momentum states inside a cavity in real time. Furthermore, due to the inefficient coupling between atomic momentum modes as we just mentioned, the matter-wave bistability is very weak since most of the atomic population will remain in the zero-momentum state. In a recent work [15] where this system is theoretically examined, it is found that bistable behavior involving tens of photons can only transfer about 20% of the total atomic population out of the zero-momentum state (see Fig. 1 of Ref. [15]).

In contrast, in the model we considered here, the coherence between the internal atomic spin states affecting atom-light interaction is induced by the intrinsic spin-exchange interaction which represents a matter-wave analog of the four-wave mixing in nonlinear optics. An immediate advantage is that it can be independently tuned with respect to the cavity field, thereby dramatically increasing the chance of large population change among spin states at a low cavity field. Consequently, our system can exhibit very strong matter-wave bistability. This is indeed confirmed by our detailed calculations.

In summary, we have studied the mutual interaction of a spinor condensate with a single-mode cavity field. We show that the coupled cavity-spinor condensate system can display simultaneously strong optical bistability at the single-photon level and strong matter-wave bistability involving a whole condensate with macroscopic number of atoms. This opens up new opportunities to explore a diversity of new phenomena in cavity nonlinear optics with low photon numbers and many-body physics with quantum gases. Before ending, we note that the condensate depletion may become significant in the long time scale as the quantum fluctuations of the cavity can introduce excess noise to the condensate system [29]. A more careful treatment taking these effects into proper account will be left for further investigation.

This work is supported by the National Natural Science Foundation of China under Grant No. 10588402, the National Basic Research Program of China (973

Program) under Grant No. 2006CB921104, the Program of Shanghai Subject Chief Scientist under Grant No. 08XD14017, Shanghai Leading Academic Discipline Project under Grant No. B480 (W.Z.), and by the NSF (H.P., H.Y.L.), ARO (H.Y.L.), and the Welch Foundation with grant C-1669 (H.P.).

-
- [1] P. Meystre, *Atom Optics* (Springer-Verlag, New York, 2001).
 - [2] H. M. Gibbs, *Controlling Light with Light* (Academic, Orlando, Fla., 1985).
 - [3] C. J. Hood *et al.*, Phys. Rev. Lett. **80**, 4157 (1998).
 - [4] A. Boca *et al.*, Phys. Rev. Lett. **93**, 233603 (2004).
 - [5] V. B. Braginsky, Y. I. Vorontsov, and K. S. Thorne, Science **209**, 547 (1980).
 - [6] F. Brennecke *et al.*, Nature **450**, 268 (2007).
 - [7] Y. Colombe *et al.*, Nature **450**, 272 (2007).
 - [8] S. Slama, *et al.*, Phys. Rev. Lett. **98**, 053603 (2007).
 - [9] S. Gupta *et al.*, Phys. Rev. Lett. **99**, 213601 (2007).
 - [10] K. W. Murch *et al.*, Nature Phys. **4**, 561 (2008).
 - [11] F. Brennecke *et al.*, Science **322**, 235 (2008).
 - [12] M. G. Moore and P. Meystre, Phys. Rev. A **59**, R1754 (1999); M. G. Moore, O. Zobay and P. Meystre, Phys. Rev. A **60**, 1491 (1999).
 - [13] P. Horak, S. M. Barnett, and H. Ritsch, Phys. Rev. A **61**, 033609 (2000); P. Horak and H. Ritsch, Phys. Rev. A **63**, 023603 (2001).
 - [14] J. Larson *et al.*, Phys. Rev. Lett. **100**, 050401 (2008).
 - [15] J. M. Zhang *et al.*, Phys. Rev. A **79**, 033401 (2009).
 - [16] T.-L. Ho, Phys. Rev. Lett. **81**, 742 (1998); T. Ohmi and K. Machida, J. Phys. Soc. Jap. **67**, 1822 (1998).
 - [17] C. K. Law, H. Pu, and N. P. Bigelow, Phys. Rev. Lett. **81**, 5257 (1998); H. Pu *et al.*, Phys. Rev. A **60**, 1463 (1999); H. Pu, S. Raghavan, and N. P. Bigelow, Phys. Rev. A **61**, 023602 (2000).
 - [18] D. R. Romano and E. J. V. de Passos, Phys. Rev. A **70**, 043614 (2004).
 - [19] W. Zhang *et al.*, Phys. Rev. A **72**, 013602 (2005).
 - [20] J. Stenger *et al.*, Nature **396**, 345 (1998).
 - [21] T. Kuwamoto *et al.*, Phys. Rev. A **69**, 063604 (2004).
 - [22] H. Schmaljohann *et al.*, Phys. Rev. Lett. **92**, 040402 (2004).
 - [23] M.-S. Chang *et al.*, Nature Phys. **1**, 111 (2005).
 - [24] A. T. Black *et al.*, Phys. Rev. Lett. **99**, 070403 (2007); Y. Liu *et al.*, Phys. Rev. Lett. **102**, 125301 (2009).
 - [25] W. Zhang, S. Yi, and L. You, New J. Phys. **5**, 77 (2003).
 - [26] The dimensionless parameters are estimated with experimentally accessible parameters: $\kappa \sim 2\pi \times 20$ KHz [8] and $N\lambda_a \sim 2\pi \times 20$ Hz for sodium atoms with a typical density 10^{14} cm⁻³ [24], $q \sim 2\pi \times 40$ Hz and $U_0 \sim -2\pi \times 100$ Hz.
 - [27] Z. P. Karkuszewski, K. Sacha, and A. Smerzi, Eur. Phys. J. D **21**, 251 (2002); B. Wu and J. Liu, Phys. Rev. Lett. **96**, 020405 (2006).
 - [28] H. Y. Ling *et al.*, Phys. Rev. A **63**, 053810 (2001); H. Y. Ling, Phys. Rev. A **65**, 013608 (2001).
 - [29] G. Szirmai, D. Nagy, and P. Domokos, Phys. Rev. Lett. **102**, 080401 (2009).